International Journal of Signal Processing, Image Processing and Pattern Recognition
Vol.8, No.9 (2015), pp.141-150
http://dx.doi.org/10.14257/ijsip.2015.8.9.14

Spectral Color Reproduction from CIE Tristimulus Values Using a Node Address Array Selection Technique

Guangyuan Wu, Zhen Liu* and Jianqing Zhang

University of Shanghai for Science and Technology, Shanghai 200093, China
wgy19882000@163.com, lunaprint@163.com, printzhangjq@126.com

Abstract

This study proposes a feasible method for spectral color reproduction based on a node address array selection technique from CIE tristimulus values. In this method three-dimensional lookup table (3-D LUT) has been constructed to connect the node address array and the spectrum as the source and destination spaces. First we present a general framework for how to reproduce spectral color. Then results of recovery are evaluated by the root mean square error (RMSE) and the color difference CIE ΔE00. According to the results considered, the proposed method could reconstruct the spectral reflectance with a high spectral and colorimetric accuracy.

Keywords: *Spectral color reproduction, Node address array, CIE tristimulus values, Spectral gamut mapping*

1. Introduction

The spectral reflectance is define as an object "fingerprinting" that accurately carry the fundamental color information, so spectral color reproduction could match original under arbitrary illuminants and observers[1-3]. However, a high-dimensional spectral data need large storage space and computational complexity. In addition, spectral color reproduction demands new approaches involving spectral-image processing, gamut boundary description and spectral gamut mapping in many applications such as textile color, art reproduction, printers with inks[3-6], so it is necessary to construct transformation chains that deliver high-quality results quickly.

In the quest for an optimal spectral color reproduction, an impressive number of spectral reproduction models have been proposed in the literature, and models are classified into two typed of categories. The first type is the analytical model algorithm that applies certain constrained optimization methods to find suitable device control values to be printed [7-9]. This discussion started with early models proposed in the 1930s by Murray, followed by Neugebauer, Yule and Nielsen, and other much more recent model forms [7]. Among all the existing models, the cellular Yule-Nielsen spectral Neugebauer (CYNSN) model was probably the most remarkable one because of its intuition and accuracy [9]. It defined the relationship between the input device control values and the output reflectance spectrum, which predicted physical properties of the printer. Printers are typically characterized by printing and measuring some samples, and setting up a "forward model" that predicts the print reflectance spectrum corresponding to each ink mixture. The more useful model form is an inverse process termed "backward modeling", which aims to invert the "forward model" by certain constrained optimization algorithms and find suitable device control values for the reflectance spectrum to be printed. Because of its cellular structure, an analytical model is effective with the advantages of higher spectral and colorimetric representing accuracy, fewer samples required[10]. However, the backward modeling cannot easily find cell that the target color is located in, which leads to time consuming.

ISSN: 2005-4254 IJSIP

The second type called lookup table (LUT) model is used to speed up the search [11-13]. LUT can be set up based on pre-collected data largely, which can eliminate calculation bottleneck in image reproduction process. To improve the spectral and colorimetric reproduction accuracy, the operations are typically implemented by increasing the sampling density. However, this operations are always time consuming to be printed and to be measured, and paper and ink need to be used leading to increase cost. In addition, spectral image usually built a high-dimensional nonlinear lookup table. Since LUT computational cost depend on LUT size, spectral color recovery from tristimulus values has become increasingly active [14, 15]. But irrespective of the previous research on colorimetric based LUTs there has been no successful research that built a 3-D LUT within a spectral color management system and evaluated the reproduction accuracies using a multicolor printer designed for spectral color reproduction.

The paper presented a method for spectral color reproduction from CIE tristimulus values by using node address array selection technique. The 3-D LUT has been constructed that achieve spectral gamut mapping. The method is used for recovery of spectral data of the GretagMacbeth ColorChecker color chips from the color coordinates of samples under a given set of illuminant-viewing conditions. The evaluations were conducted by calculation of color difference values under different illuminants and RMS errors between the original and the reconstructed spectra.

2. Materials and Methods

2.1 Step 1: Cellular Yule-Nielsen Spectral Neugebauer (CYNSN)

The CYNSN model has been widely adopted in printer forward modeling workflows, because its cellular structure enhances the model prediction accuracy remarkably. A forward model is an efficient way to correct the problem caused by nonlinearity between the measured and predicted reflectances, so the relationship between the input device control values and the output reflectance spectrum is calculated efficiently and accurately.

The classical Yule-Nielson Spectral Neugebauer model is an exponential correction modified spectral Neugebauer model, accounting for optical and physical paper and ink interactions. It can be described as

$$R(\lambda) = \left(\sum_{i=1 \to N} w_i R_i(\lambda)^{1/n} \right)^n \tag{1}$$

where $R(\lambda)$ is the predicted reflection spectrum; $R_i(\lambda)$ is the spectral reflectance of the ith Neugebauer primary; i denotes the number of Neugebauer primaries and $N = 2^i$; n is the coefficient of the power function, known as the Yule-Nielson *n*-factor; w_i is defined by the Dmichel equation, dependent on the normalized ink amount values of the color target.

$$w_i = \prod_{j=1 \to i} \begin{pmatrix} a_j & If\ ink\ j\ is\ in\ Neugebbauer\ primary\ i \\ 1 - a_j & If\ ink\ j\ is\ not\ in\ Neugebauer\ primary\ i \end{pmatrix} \tag{2}$$

where a_j denotes the surface coverage of primary color j. To improve the spectral and colorimetric prediction accuracy, a well-known model called the cellular Yule-Nielson spectral Neuebauer (CYNSN) model subdivides the device space into cellular regions to obtain more sub-models and primaries. Equation was applied on each cell. Prior to this, in each cell, the amount values of the colorant were renormalized to the range of 0-1. Normally, the more cellular levels used, the higher the accuracy obtained; however, it also brings new challenges that more samples need to be measured.

2.2 Step 2: Node Address Array-Based Lookup Table

The CIE XYZ tristimulus values of a surface with spectral $r(\lambda)$ that is viewed under an illuminant with spectral power distribution $I(\lambda)$ can be determined as

$$X = k \int r(\lambda) I(\lambda) \bar{x}(\lambda) d\lambda \tag{3}$$

$$Y = k \int r(\lambda) I(\lambda) \bar{y}(\lambda) d\lambda \tag{4}$$

$$Z = k \int r(\lambda) I(\lambda) \bar{z}(\lambda) d\lambda \tag{5}$$

with

$$k = \frac{100}{\int I(\lambda) \bar{y} d\lambda} \tag{6}$$

where $\bar{x}$, $\bar{y}$, $\bar{z}$ are the CIE color matching functions, and the integral is computed over the visible spectrum. The CIE Lab values can be converted from the XYZ space using inverse CIE equations.

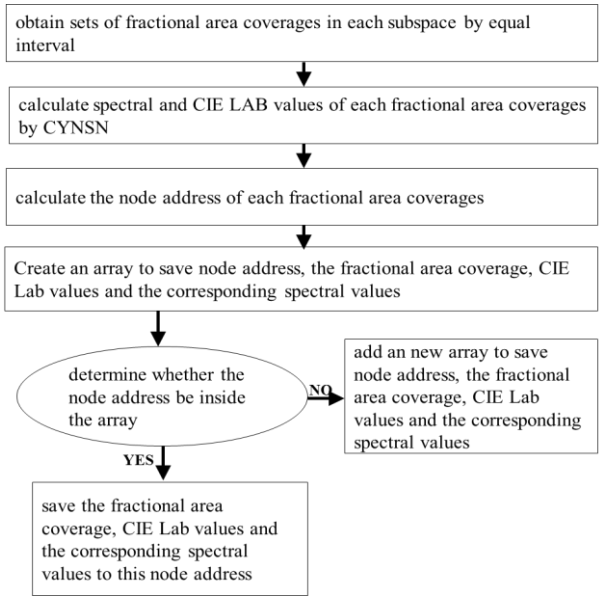

Figure 1. Schematic Diagram for Using Node Address Array based on Spectral Printer Model

The node address array selection technique can be classified as statistical methods and can be used in the color engineering [16]. This method is usually employed for grouping objects, so it has features of better performance and low computational complexity. In Figure 1, the steps for describing the spectral gamut using node address array based on spectral printer model are illustrated. First, sub-models of the spectral gamut adopted equal interval sampling, so that it obtained sets of fractional area coverages in each subspace. After spectral and CIE LAB values of each fractional area coverage could be calculated by CYNSN of each sub-model. The node address array could be calculated by CIE Lab using to describe the spectral gamut of the printer. Then, a node address array was created using to store data including the node address, the fractional area coverage, CIE Lab values and the corresponding spectral values. Finally, during the process of describing the spectral gamut, each node address in the sets determined whether the node address is inside the array. If it was, the fractional area coverage, CIE Lab values and the

corresponding spectral values save this node address array. If not, it means that the new node address array needed to be added to save the node address, the fractional area coverage, CIE Lab values and the corresponding spectral values.

A node address from the CIE Lab as used herein follows the algorithms below:

$$L_{node\_address} = round(L/n_L) \quad (7)$$

$$a_{node\_address} = round(a/n_a) \quad (8)$$

$$b_{node\_address} = round(b/n_b) \quad (9)$$

where n_L, n_a, n_b are the interval of each axis in the CIE Lab.

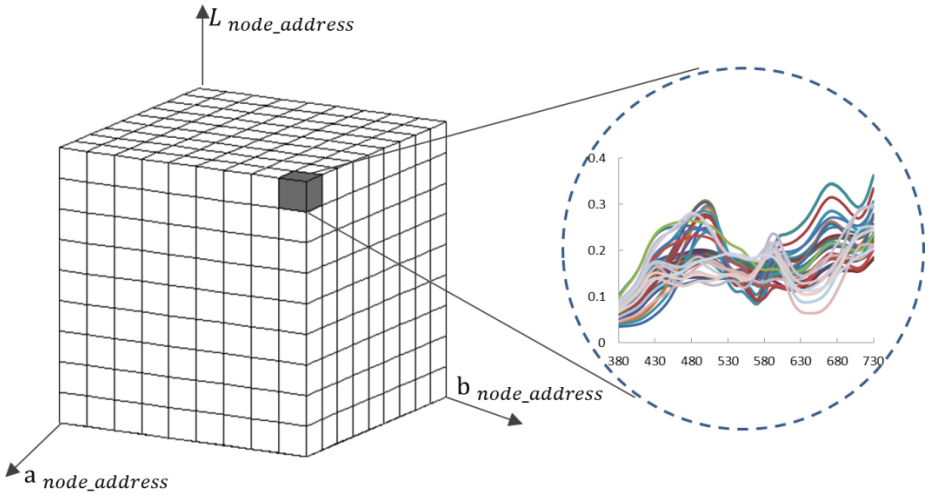

Figure 2. Three-dimensional LUT based on Node Address Array Selection Technique

A three-dimensional LUT based on node address array selection technique from CIE tristimulus values is illustrated in Figure 2. For purposes of illustration, the LUT is divided into two portions: node addresses LAB and spectral subset. Each sub-cube in the node address LAB portion is considered to hold spectral subset containing sets of spectral reflectances and the corresponding fractional area coverages.

2.3 Step 3: Spectral Gamut Mapping

In the process of spectral color reproduction, spectral gamut mapping is necessary since an answer must be delivered for any arbitrary spectral request, even those outside of a printer's spectral gamut.[12] To our knowledge one spectral color is outside the spectral gamut of a printer when the corresponding CIE Lab is outside the color gamut of the printer. Figure 3 describes the steps for the spectral gamut mapping. First, the node address and the CIE Lab values were computed from the input spectral reflectance. Then, the node address was determined whether the node address is inside the array. If it was, the errors were calculated between the input spectral reflectance and each spectrum of the spectral subset, and the optimal spectral and fractional area coverages were chose by the spectral quality evaluating metrics. If not, the corresponding CIE Lab values chose the mapping point of the smallest color difference in all samples set, and the node address of the mapping point is necessarily inside the color gamut of the printer.

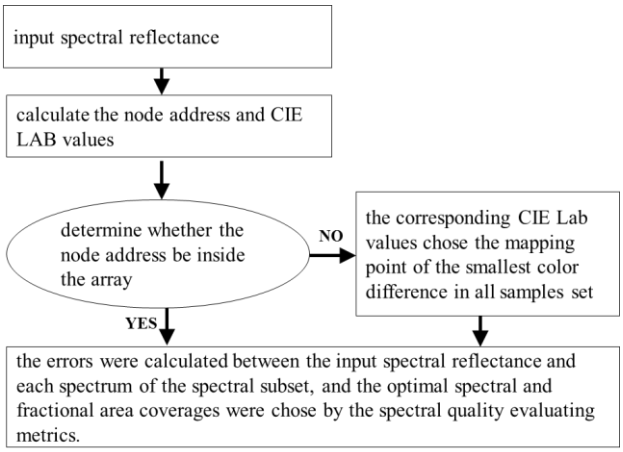

Figure 3. Schematic Diagram for the Spectral Gamut Mapping

This paper is based on some accepted rational and practical principals. Our summarized the principals as follow:

(1) One spectral color is outside the spectral gamut of a printer when the corresponding CIE Lab is outside the color gamut of the printer.

(2) Spectral consists of colorimetric values and metameric blacks under a particular viewing condition [3, 17].

(3) Similar colorimetric values and spectral values save the same node address array.

(4) If one spectral color is inside the spectral gamut of a multichannel printer, it can be reasonable approximated by a certain set (i.e., of three or four) of carefully chosen inks for the printer [18].

3. Experiment and Analysis

A HP Designjet Z3200 inkjet printer with a customized control driver was spectrally characterized for printer simulation. This printer had the capability of a twelve-color ink set, but only seven were utilized: cyan (C), magenta (M), yellow (Y), black (K), red (R), green (G) and blue (B). The EFI Colorproof XF software was used to normalize the ink amount values, and all sample sets were printed out under this normalization workflow. All samples were printed on EasiColor EP520 210g SemiMatt proofing paper, and the print resolution of the ink jet printer was 1200 by 1200 dpi. An X-rite i1iO spectrophotometer was used for spectral measurements of the printed samples, and sampled at spectral wavelengths from 400 to 700 nm in 10nm intervals.

The role of forward CYNSN model was to locate the cell that given color was located in by ink mount values of the given color and to predict the corresponding spectral reflectance. The more gird points used, the better the CNSYS model performance became. The performance for different number of grid points had been proven by several studies [9,10,19]. With a trade-off between the computational cost and the resulting accuracies, this paper chose the six-grid-point CYNSN as the forward model.

Printer subdivision is a commonly used approach in spectral printer models, and the feasibility has been proven by several studies [9,10,19,20]. However, to our knowledge litter research has been studied about the influence of different printer subdivision method to the global gamut of the printer. In this paper, we still rely on Wang's subdivision method[19] and consider to be the maximum gamut for a multi-channel printer, so a CMYKRGB printer divided into 5 four-ink sub-models including black (CGYK, YRMK, MBCK, CMYK, RGBK) and 3 three-ink sub-models (BCG, GYR, RMB). The training sample set consists of 7128 color patches shows was printed out with five steps of 0, 0.2, 0.4, 0.6, 0.8, 1 in each of printer subdivision color coordinates. Testing sample set which

consists of 3500 color patches shows was printed out with five steps of 0, 0.25, 0.5, 0.75 , 1 in each of printer subdivision color coordinates. The printer model achieved sufficient prediction accuracies: an average CIEDE2000 of 0.4786; and average spectral RMS error of 0.0037. With a trade-off between the computational cost and the resulting accuracies, n_L, n_a, n_b were chose 6, 18, 18; and the interval of the fractional area coverage in the node address array lookup table was chose 11 level for every sub-models.

By use of the GretagMacbeth ColorCheck, the performance of spectral color reproduction using different metrics using a node address array selection technique were presented in Table 1. The root mean square error (RMSE) had been used for evaluating the spectral predicting accuracy, and the CIE2000 formula, denoted as ΔE00, was adopted to represent the colorimetric predicting accuracy. In consideration of the metamerism problem, colorimetric values were calculated under four different illuminants (A, D50, D65 and F1) for the CIE 1931 2°standard observer. Meanwhile, since the root mean square error (RMSE) can easily switch between the spectral and colorimetric reproduction intent without the need for repeat modeling, all the modeling procedure proceeded on the basis of RMSE minimization. As can be seen in Table 1, the average prediction accuracy of our proposed method could achieve the high spectral and colorimetric representing accuracy, which tended to provide somewhat robust color matching.

Table 1. Performance of Spectral Color Reproduction Using Different Metrics

	Max	Mean	Median
RMSE	0.0590	0.0320	0.0297
ΔE00(A)	4.8744	2.4568	2.1493
ΔE00(D50)	7.9967	3.0355	2.7238
ΔE00(D65)	6.6128	2.9786	2.7748
ΔE00(F1)	5.4119	3.1992	2.9882

To further demonstrate the performance of our presented method, more detailed information about the reproduction for the ColorChecker was presented in Figure 4. This figure illustrated the spectral accuracy of the RMSE for the ColorChecker. It was obvious here that the method presented the high spectral accuracy. The smaller the RMSE was, the closer the original reflectance became. Only Nos. 12, 16 and 17 of the RMSE values exceeded 0.05, but the maximum value less than 0.06. Figure 5 show the maximum spectral RMS error of the ColorChecker.

Figure 6 show the colorimetric reproduction accuracy of the ColorCecker under four typical illuminants. Generally speaking, most of values are less than 5, our method achieve the high colorimetric accuracy. Figure 7 show the maximum ΔE00 of the ColorChecker. From Figure 5 and 7, the model could not reproduce the spectral curve shape where the reflectance changed sharply; the main reason is that only seven inks were utilized in this research.

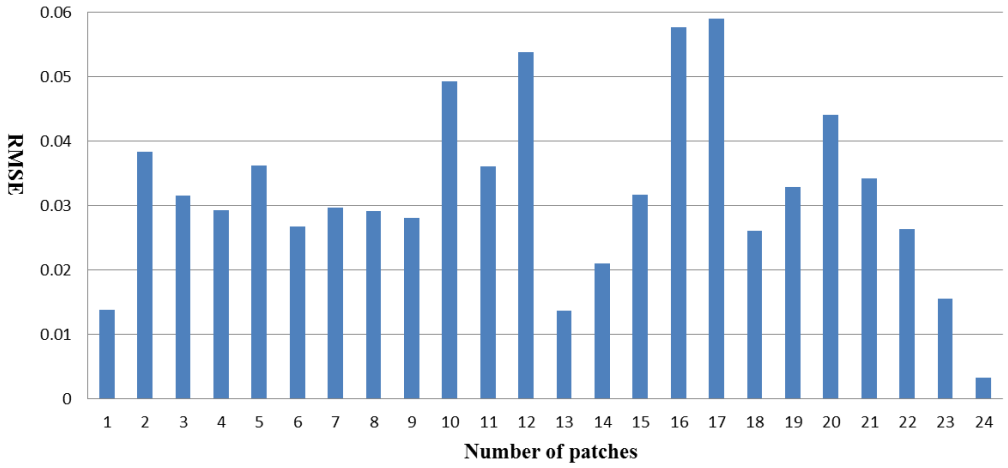

Figure 4. Spectral Accuracy (RMSE) of the ColorChecker Reproduction for Minimizing RMSE

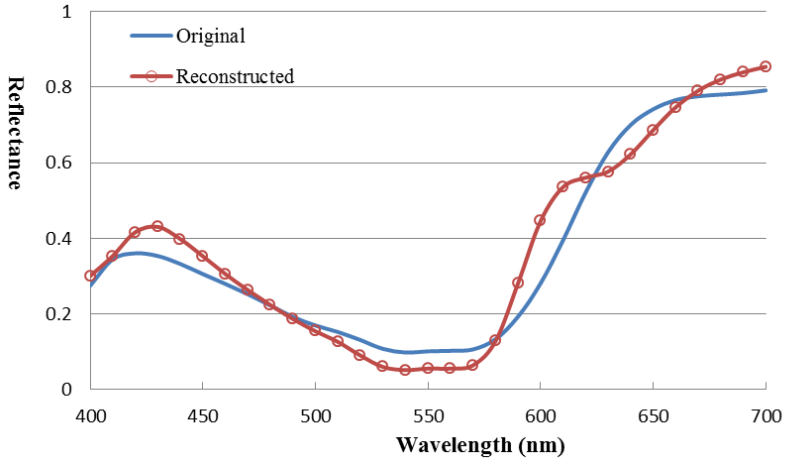

Figure 5. Spectral Reproduction of the Patch No. 17 using RMSE Minimization

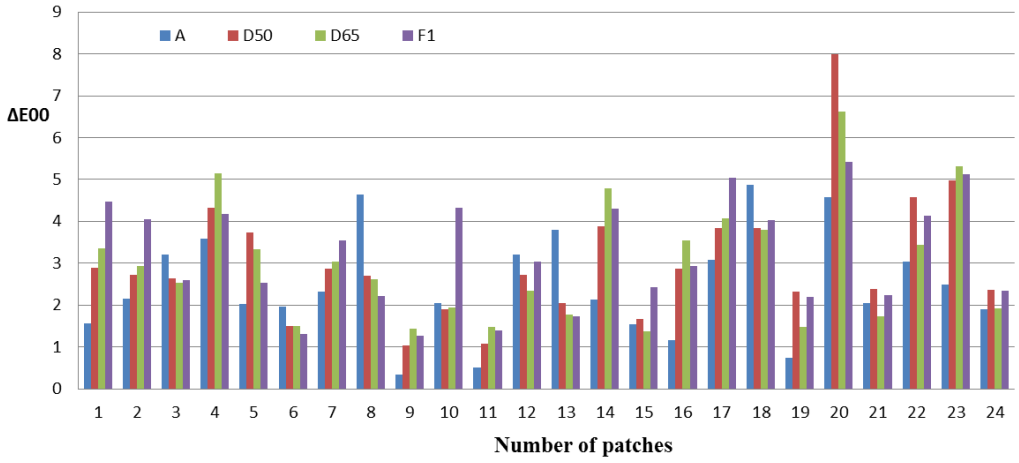

Figure 6. Colorimtric Accuracy (ΔE00) of the ColorChecker Reproduction for Minimizing RMSE

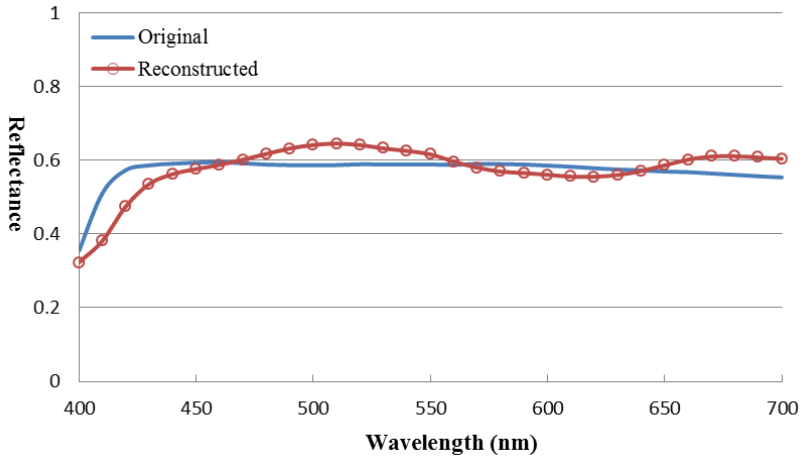

Figure 7. Spectral Reproduction of the Patch No. 20 using RMSE Minimization

4. Conclusion

Spectral color reproduction from CIE tristimulus values using a node address array selection technique has been demonstrated. The three-dimensional lookup table (3-D LUT) has been constructed to connect the node address array and the spectrum as the source and destination spaces, which achieves spectral gamut mapping. The reflectance spectrum of the ColorCheck is used as samples in this research. Different error metrics have been considered to assess the performances of the proposed method: the RMSE and the color different CIE ΔE00 under four different illuminants (CIE A, D50, D65 and F1). According to the results considered, the proposed method could achieve a high spectral and colorimetric accuracy for spectral color reproduction.

Acknowledgements

This study was supported by the National Natural Science Foundation of China (no.41271446) and the Innovation Fund Project for Graduate Student of Shanghai (no.JWCXSL1401).

References

[1] H. L. Shen and J. H. Xin, "Estimation of spectral reflectance of object surfaces with the consideration of perceptual color space," Optics Letters, vol. 32, no. 1, (**2007**), pp. 96-98.
[2] X. Zhang, Q. Wang, Y. Wang and H. Wang, "XYZLMS interim connection space for spectral image compression and reproduction," Optics Letters, vol. 37, no. 24, (**2012**), pp. 5097-5099.
[3] S. Tsutsumi, M. R. Rosen and R. S. Berns, "Spectral Gamut Mapping using LabPQR," Journal of Imaging and Technology, vol. 51, no. 6, (**2007**), pp. 473-485.
[4] J. Mohtasham, A. S. Nateri and H. Khalili, "Textile colour matching using linear and exponential weighted principal component analysis," Coloration Technology, vol. 128, no. 3, (**2012**), pp. 199-203.
[5] E. M. Valero, Y. Hu, J. Hernández-Andrés, T. Eckhard, J. -L. Nieves, J. Romero, M. Schnitzlein and D. Nowack, "Comparative performance analysis of spectral estimation algorithms and computational optimization of a multispectral imaging system for print inspection," Color Research and Application, vol. 39, no. 1, (**2014**), pp. 16-27.
[6] H. Haneishi, T. Hasegawa, A. Hosoi, Y. Yokoyama, N. Tsumura and Y. Miyake, "System Design for Accurately Estimating the Spectral Reflectance of Art Paintings," Applied Optics, vol. 39, no. 35, (**2000**), pp. 66621-6632.
[7] D. R. Wyble and R. S. Berns, "A critical review of spectral models applied to binary color printing," Color Research and Application, vol. 25, no.1, (**2000**), pp. 4-19.
[8] T. Bugnon andR. D. Hersch, "Recovering neugebauer colorant reflectances and Ink-spreading curves from printed color images," Color Research and Application, vol. 39, no.3, (**2014**), pp. 216-233.

[9] Q. Liu, X. Wan and D. Xie, "Optimization of spectral printer modeling based on a modified cellular Yule-Nielsen spectral Neugebauer model," Journal of the Optical Society of America A, vol. 31, no. 6, (**2014**), pp. 1284-1294.
[10] J. Guo, H. Xu and M. R. Luo, "Novel spectral characterization method for color printer based on the cellular Neugebauer model," Chinese Optics Letters, vol. 8, no. 11, (**2010**), pp. 1106-1109.
[11] J. Mielikainen, "Lossless compression of hyperspectral images using lookup tables," Signal Processing Letters, IEEE, vol. 13, no. 3, (**2006**), pp. 157-160.
[12] S. Tsutsumi, M. R. Rosen and R. S. Berns, "Spectral Color Reproduction using an Interim Connection Space-Based Lookup Table," Journal of Imaging Science and Technology, vol. 52, no. 4, (**2008**), pp. 4020-1-13.
[13] R. Balasubramanian, "Reducing the cost of lookup table based color transformations," Journal of Imaging Science Technology, vol. 44, no. 4, (**2000**), pp. 321-327.
[14] B. G. Kim, J. Han and S. Park, "Spectral Reflectivity Recovery from the Tristimulus Values using a Hybrid Method," Journal of the Optical Society of America A, vol. 29, no. 12, (**2012**),pp. 2612-2621.
[15] D. Wu, J. Tian and Y. Tang, "Optimized Basis Function for Spectral Reflectance Recovery from Tristimulus Vales," Optical Review, vol. 21, no. 2, (**2014**), pp. 117-126.
[16] M. Zhu, Z. Liu and G. Chen, "Research on six-color separation model based on subarea neugebauer equations," Acta Optica Sinica, vol. 31, no. 7, (**2011**), pp. 0733001-1-10.
[17] Y. Zhao and R. S. Berns, "Image-Based Spectral Reflectance Reconstruction using the Matrix R Method," Color Research and Application, vol. 32, no. 5, (**2007**), pp. 343-351.
[18] D. Tzeng, "Spectral-based color separation algorithm development for multi-ink color reproduction," Ph.D. dissertation (Rochester Institute of Technology, (**1999**).
[19] B. Wang, H. Xu and M. R. Luo, "Color separation criteria for spectral multi-ink printer characterization," Chinese Optics Letters, vol. 10, no. 1, (**2012**), pp. 013301-1-4.
[20] B. Wang, H. Xu, M. R. Luo and J. Guo, "Spectral-based color separation method for a multi-ink pinter," Chinese Optics Letter, vol. 9, no. 6, (**2011**), pp. 063301-1-4.

